



H_∞ Feedback Control for Switched Linear Systems: Application to an Engine Air Path System

Caroline Ngo, Damien Koenig, Olivier Sename, H Béchart

► To cite this version:

Caroline Ngo, Damien Koenig, Olivier Sename, H Béchart. H_∞ Feedback Control for Switched Linear Systems: Application to an Engine Air Path System. IFAC WC 2014 - 19th IFAC World Congress, Aug 2014, Le Cap, South Africa. hal-01084851

HAL Id: hal-01084851

<https://hal.science/hal-01084851>

Submitted on 20 Nov 2014

HAL is a multi-disciplinary open access archive for the deposit and dissemination of scientific research documents, whether they are published or not. The documents may come from teaching and research institutions in France or abroad, or from public or private research centers.

L'archive ouverte pluridisciplinaire **HAL**, est destinée au dépôt et à la diffusion de documents scientifiques de niveau recherche, publiés ou non, émanant des établissements d'enseignement et de recherche français ou étrangers, des laboratoires publics ou privés.

H_∞ State Feedback Control for Switched Linear Systems: Application to an Engine Air Path System

C. Ngo * D. Koenig ** O. Sename ** H. Béchart *

* Renault, 1 Avenue du Golf, TCR LAB 0 12, 78084 Guyancourt Cedex, FRANCE (e-mail: (caroline.ngo, hubert.bechart)@renault.com)

** GIPSA-Lab, Grenoble INP - Université Joseph Fourier, 11 rue des Mathématiques, BP46, 38402 Saint Martin D'Hères Cedex, FRANCE (e-mail: (damien.koenig, olivier.sename)@gipsa-lab.grenoble-inp.fr)

Abstract: This paper presents the results of an engine air-path H_∞ state feedback switched linear controller. The main advantage of this approach is that controller gains are calculated offline, with the robust specifications allowing fast calculation and is cost-effective in calculation and resources.

The air-path system dynamics are governed by the Saint-Venant equations, difficult to handle in control synthesis due to its nonlinear properties (states - control inputs coupling, nonlinear functions). To employ advanced control techniques, a switched linear state space representation is proposed. The model is simplified considering that slow dynamics are quite constant. The proposed approach provides a robust state feedback control toward perturbations (model error, unmodeled dynamics...) by considering these disturbances as unknown inputs.

Keywords: Linear systems; Robust control; Process control

1. INTRODUCTION

Nowadays, severe norms impose car manufacturer strict pollutant emission regulations (like EURO normative in Europe). To meet future pollutant emission standards and customer request of performances (fuel consumption reduction with the same engine power), manufacturers need to develop new technologies, but also more sophisticated engine control strategies. A promising way to achieve this goal is the engine downsizing, reducing fuel consumption without degrading final delivered power. Additional systems such as supercharger or turbocharger, electronic actuators (for example, throttle valve or Variable Valve Timing) complicate the air path system of downsized engines, where more and more advanced control techniques have to be involved.

During the last decade, the air path system has become a crucial part in engine development. Indeed, air path control is strongly linked to engine performances, since torque is directly related to the injected air quantity, and also on engine pollutant emission control. The objective of the air path control is to provide the driver's torque request while injecting accurate amount of mass flow air, and so pressure to ensure pollutant emission control.

The air-path system dynamics are governed by the Saint-Venant equation, difficult to handle in control synthesis due to its nonlinear properties (states - control inputs coupling, nonlinear functions). To manage these nonlinear equations, many use nonlinear techniques using several methods: input-state linearization controller as in Moulin

and Chauvin [2008] or Leroy et al. [2008], predictive control as in Iwadare et al. [2009]. Authors in Moulin and Chauvin [2008] present a strategy consisting of constrained motion planning and feedback linearization but properties of the closed loop system (convergence, stability, constraints) are harder to prove. In Nguyen et al. [2012b], the control is based on Takagi-Sugeno (TS) model. Such an approach is interesting to cope with nonlinear systems, since, using the sector nonlinearity concept, the TS model is a convex combination of local linear models where the non linearities are included in the membership functions. However, such approach is still heavy to implement since nonlinear functions are still present.

In this article, a H_∞ state feedback switched linear controller is proposed, providing robustness to perturbations (disturbances, unmodeled dynamics...) by considering these disturbances as unknown inputs. It is important to note that the switching control approach is completely linear and easy to handle and to implement in a car embedded controller. Even if this approach seems rather similar to the TS one presented in Nguyen et al. [2012a], no nonlinear membership functions have to be computed in switching control, which makes this approach interesting in the case of low-cost systems design where cost calculator constraints limit the use of computing resources. Here, the study is focused on the control of the intake air path system of a Spark-Ignition (SI) engine, composed of a throttle valve, a supercharger with a bypass valve.

The paper is organized as follows. In section 2 the nonlinear model of the air path system is presented. A switched

linear state space representation is proposed from the Saint-Venant equations. This model has been validated on simulation results. In section 3, a robust H_∞ switched linear controller is designed by solving multiple Linear Matrix Inequality (LMI) and the obtained gains guarantee the stability and the robust specification whatever the switching sequence, and section 4 is devoted to the simulation results of this air-path switching control on a nonlinear model.

Notations: $(\cdot)^T$ stands for transpose matrix, $(\cdot) > 0$ denotes a positive definite matrix and $(*)$ stands for symmetric terms.

2. SPARK IGNITION ENGINE AIR-PATH SYSTEM

The quantity of air injected to the cylinder during a motor cycle is delivered by the air-path system. The studied system is an spark-ignition engine air-path composed of a throttle valve and a supercharger equipped with a bypass valve.

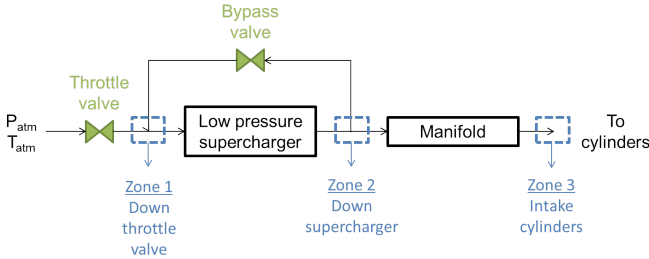


Fig. 1. Studied air path system architecture

The throttle valve adjusts the intake mass flow by varying the throttle valve angle, i.e. the effective opening area. The supercharger speed is proportional to the engine speed, and increases the intake air pressure. The supercharger is equipped of a bypass valve, which is actuated when intake supercharger pressure is less than the one at his outlet to avoid surge situation. In the studied case, the difficulty for control synthesis is to take into account of the supercharger dynamics, since the supercharger is located after the throttle valve (see Fig.1).

2.1 Supercharged Air System Model

The presented model is obtained from energy conservation law and Saint-Venant equation giving the mass flow rate through a section (see Heywood [1988], Guzzella and Onder [2004]).

The pressure dynamics along the air path are governed by the following non linear equations:

$$\begin{aligned}\dot{P}_1 &= \frac{rT_1}{V_1} [Q_{thr} - Q_{comp} + Q_{byp}] \\ \dot{P}_2 &= \frac{rT_2}{V_2} [-Q_{byp} - Q_{man} + Q_{comp}] \\ \dot{P}_3 &= \frac{rT_3}{V_3} [Q_{man} - Q_{cyl}]\end{aligned}$$

With: P_i , the pressure, T_i , the temperature, V_i , the volume and Q_i , the mass flow rate.

Notations:

1,2,3 stand for the volumes after throttle valve, after supercharger and before intake cylinder, resp.

thr, byp, comp, man, cyl denote resp. the throttle, the bypass, the supercharger, the manifold (before intake cylinder) and the intake cylinder.

The mass flow rates Q_i are given by the Saint-Venant equations:

Q_{comp} is obtained by an experimental 2D lookup table.

Throttle: $Q_{thr}, X = \frac{x_1}{P_{atm}}$	
$X > X_c$	$A_{thr} \frac{P_{atm}}{\sqrt{rT_{atm}}} \left(\frac{x_1}{P_{atm}}\right)^{\frac{1}{\gamma_c}} \sqrt{\frac{2\gamma_c}{\gamma_c-1} \left(1 - \left(\frac{x_1}{P_{atm}}\right)^{\frac{\gamma_c-1}{\gamma_c}}\right)}$
$X \leq X_c$	$A_{thr} \frac{P_{atm}}{\sqrt{rT_{atm}}} \left(\frac{2}{\gamma_c+1}\right)^{\frac{1}{\gamma_c-1}} \sqrt{\frac{2\gamma_c}{\gamma_c-1} \left(1 - \frac{2}{\gamma_c+1}\right)}$
Bypass: $Q_{byp}, X = \frac{x_1}{x_2}$	
$X > X_c$	$A_{byp} \frac{x_2}{\sqrt{rT_2}} \left(\frac{x_1}{x_2}\right)^{\frac{1}{\gamma_c}} \sqrt{\frac{2\gamma_c}{\gamma_c-1} \left(1 - \left(\frac{x_1}{x_2}\right)^{\frac{\gamma_c-1}{\gamma_c}}\right)}$
$X \leq X_c$	$A_{byp} \frac{x_2}{\sqrt{rT_2}} \left(\frac{2}{\gamma_c+1}\right)^{\frac{1}{\gamma_c-1}} \sqrt{\frac{2\gamma_c}{\gamma_c-1} \left(1 - \frac{2}{\gamma_c+1}\right)}$
Manifold: $Q_{man}, X = \frac{x_3}{x_2}$	
$X > X_c$	$A_{man} \frac{x_2}{\sqrt{rT_2}} \left(\frac{x_3}{x_2}\right)^{\frac{1}{\gamma_c}} \sqrt{\frac{2\gamma_c}{\gamma_c-1} \left(1 - \left(\frac{x_3}{x_2}\right)^{\frac{\gamma_c-1}{\gamma_c}}\right)}$
$X \leq X_c$	$A_{man} \frac{x_2}{\sqrt{rT_2}} \left(\frac{2}{\gamma_c+1}\right)^{\frac{1}{\gamma_c-1}} \sqrt{\frac{2\gamma_c}{\gamma_c-1} \left(1 - \frac{2}{\gamma_c+1}\right)}$
Cylinder: $Q_{cyl}, X = \frac{P_{cyl}}{x_3}$	
$X > X_c$	$A_{cyl} \frac{x_3}{\sqrt{rT_3}} \left(\frac{P_{cyl}}{x_3}\right)^{\frac{1}{\gamma_c}} \sqrt{\frac{2\gamma_c}{\gamma_c-1} \left(1 - \left(\frac{P_{cyl}}{x_3}\right)^{\frac{\gamma_c-1}{\gamma_c}}\right)}$
$X \leq X_c$	$A_{cyl} \frac{x_3}{\sqrt{rT_3}} \left(\frac{2}{\gamma_c+1}\right)^{\frac{1}{\gamma_c-1}} \sqrt{\frac{2\gamma_c}{\gamma_c-1} \left(1 - \frac{2}{\gamma_c+1}\right)}$

Table 1. Mass flow equations at different sections of the air system

with:

A_{thr} , throttle opening effective area, depends on the valve opening angle $\theta_{thr} = u_1$.

A_{byp} , bypass effective opening area, depends on the valve opening angle $\theta_{byp} = u_2$.

A_{man} , manifold effective area.

A_{cyl} , mean intake cylinder effective area.

X_c , critical pressure ratio: $X_c = \left(\frac{2}{\gamma_c+1}\right)^{\frac{\gamma_c}{\gamma_c-1}}$

γ_c , heat capacity ratio: $\gamma_c = \frac{c_p}{c_v}$

r , gas constant.

Finally, the temperatures are given by the following expressions which have been obtained by assuming that temperature dynamics are slow compared to the pressures dynamics, so:

$$\dot{T}_1 = \dot{T}_2 = \dot{T}_3 = 0$$

Leading to:

$$\begin{aligned}
T_1 &= 300K \\
T_2 &= \frac{T_1 \beta_{comp}(x_1, x_2) Q_{comp} + \frac{h_2 S_2}{C_p} T_{wall}}{Q_{man} + Q_{byp} + \frac{h_2 S_2}{C_p}} \\
T_3 &= \frac{T_2 Q_{man} + \frac{h_3 S_3}{C_p} T_{wall}}{Q_{cyl} + \frac{h_3 S_3}{C_p}}
\end{aligned}$$

2.2 Switched linear representation

In order to use advanced linear control techniques, the previous model is linearized around several chosen operating points. The obtained model is written under switched linear system representation.

The switched system obtained by linearization is a practical way to take account of the two expressions of the Saint-Venant equations describing the mass flow rates.

Let consider the following discrete time switched system:

$$\begin{cases} \tilde{x}_{k+1} = \sum_{i=1}^n \alpha_i(k) (A_i \tilde{x}_k + B_i \tilde{u}_k) \\ \tilde{y}_k = C_{yi} \tilde{x}_k \\ \tilde{z}_k = C_{zi} \tilde{x}_k \end{cases} \quad (1)$$

where:

$$\begin{aligned}
A_i &= \left. \frac{\partial f(x, u)}{\partial x} \right|_{x_i, u_i}, & A_i &\in \mathbb{R}^{m \times m}, \\
B_i &= \left. \frac{\partial f(x, u)}{\partial u} \right|_{x_i, u_i}, & B_i &\in \mathbb{R}^{m \times p}, \\
C_{yi} &= C_y, & C_y &\in \mathbb{R}^{t \times m}, \\
C_{zi} &= C_z, & C_z &\in \mathbb{R}^{h \times m}, \\
\tilde{x} &= x - x_i, & x &\in \mathbb{R}^m, \\
\tilde{u} &= u - u_i, & u &\in \mathbb{R}^p, \\
\tilde{y} &= y - y_i, & y &\in \mathbb{R}^t, \\
\tilde{z} &= z - z_i, & z &\in \mathbb{R}^h
\end{aligned}$$

z is the controlled output and y is the measurement. x_i and u_i are the chosen operating points, (A_i, B_i, C_y, C_z) are the state, input, measure and control output matrices respectively, and: $x_{k+1} = f(x_k, u_k)$

In the case of switched model application on air path system, let denote:

$$x = \begin{pmatrix} P_1 \\ P_2 \\ P_3 \end{pmatrix} \quad u = \begin{pmatrix} \theta_{thr} \\ \theta_{byp} \end{pmatrix}$$

$\alpha_i(k)$ is the switching signal and satisfies the following convex properties:

$$\begin{cases} \sum_{i=1}^n \alpha_i(k) = 1 \\ 0 \leq \alpha_i(k) \leq 1 \end{cases}$$

α_i specifies which subsystem is activated at each time k . This variable is constant and equals to 0 or 1 according to switching variable value, for example, if $\alpha_i(k) = 1$, $\alpha_{j \neq i}(k) = 0$, meaning that the matrices (A_i, B_i) are activated.

One can remark in the case where the switching variable is not measured, this switched linear model can be extended with an estimation of the switching variable. This approach is presented in Ichalal et al. [2010] and Ichalal et al. [2012].

Each model represents an operating point depending on the values of the control input and the pressure ratio. In this application, the switch sequence is computed on two levels:

- According to the value of the control input, the operating points (x_j, u_j) are selected.
- Then, comparison of the pressure ratio value $X = \frac{P_{down}}{P_{up}}$ and the critical pressure ratio value of each considered section of the air path system give the adequate mass flow equation (see *Table 1*) to compute (A_i, B_i) .

The following figure illustrate how operating range are chosen with the throttle valve characteristic. The variation of the opening area is proportional to the intake pressure. We chose to fit the characteristic by tangent lines on the 5 chosen operating points.

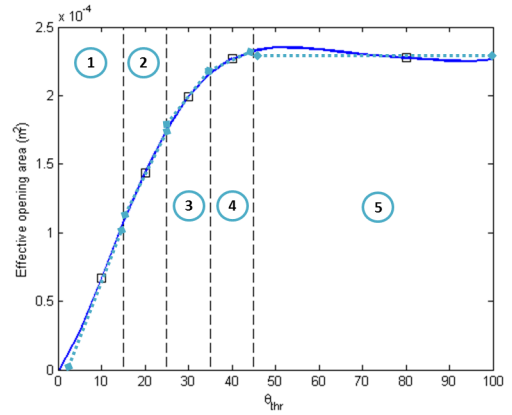


Fig. 2. Throttle valve characteristic

The switched linear model has been validated using comparison with the nonlinear model. It is important to mention that even if the nonlinear model has not been validated on experimental data, it was already validated on the engine simulation software GT-POWER.

Let $x = [P_1, P_2, P_3]$, $u = [\theta_{thr}, \theta_{byp}]$ denoting respectively the states and the control inputs. Throttle valve signal is a step between the maximum opening area percentage values of $\theta_{thr} = 5\%$ and $\theta_{thr} = 50\%$ (above 40%, pressure is quite constant), and $\theta_{byp} = 0\%$ to $\theta_{byp} = 10\%$.

Fig.3 and *Fig.4* show the results of the model validation.

Good results are obtained by this switched model although simple, the complex dynamics of the air path system on the chosen operating points are well modeled. Modelization error of the pressures remain small but tend to increase at small throttle opening value and far from the chosen operating points. Very few noise from switches is present, which is a good point for the actuators since saturation limits are not reached.

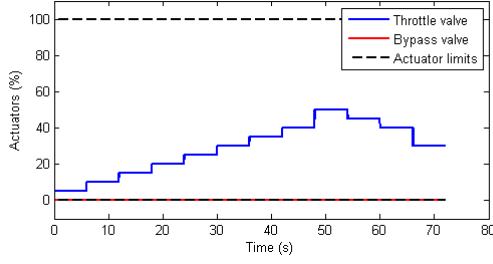


Fig. 3. Throttle (blue) and Bypass (red) valves signals from the switched linear model

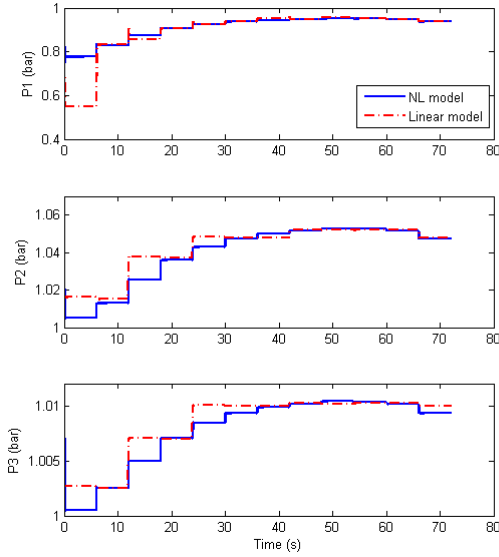


Fig. 4. Pressures comparison between non-linear model (blue solid line) and switched linear model (red dashed line) simulation

In the following, unknown inputs for controller synthesis are considered to take account of the leak of model precision at small throttle opening value and operating area far from the linearization points.

3. H_∞ STATE FEEDBACK CONTROL FOR SWITCHED LINEAR SYSTEM ROBUST TO UNKNOWN INPUTS

The main advantage of the linear switching approach is that controller gains are calculated offline, with the robust specifications allowing fast calculation and is cost-effective in calculation and resources.

The objective of this work is to provide a robust way to control the air-path system on specified operating points. The pressures along the air-path system are low, which makes robust control essential here. Indeed, many disturbances, difficult to model are present (mainly back pressures) and also modeling errors induced by the model reduction.

This section presents a way to control a disturbed air-path system with a H_∞ state feedback controller with

integrator effect to ensure reference tracking performance. In the following, the controller synthesis is done with performance analysis.

3.1 Integrator effect

Integral control is necessary to ensure zero steady-state error during tracking process. Integrator effect is obtained by extending the switched system state vector with the integrator state x^{int} :

$$x_{k+1}^{int} = x_k^{int} + t_e(z_k^{ref} - z_k) = x_k^{int} - t_e C_{zi} \tilde{x}_k \quad (2)$$

z_k^{ref} is the reference signal and t_e is the discrete system sample period.

3.2 Discrete time switched robust H_∞ state feedback controller design using Lyapunov approach

To take into account the model uncertainties or unmodeled disturbances, unknown inputs are included, the discrete time system is then described by:

$$\begin{cases} \tilde{x}_{k+1} = \sum_{i=1}^n \alpha_i(k) (A_i \tilde{x}_k + B_i \tilde{u}_k + W_i w_k) \\ \tilde{z}_k = C_{zi} \tilde{x}_k \end{cases} \quad (3)$$

where: W_i and C_{zi} denote the unknown inputs and the controlled output \tilde{z}_k matrices, respectively.

Using equations (2) and (3), the extended system is described by:

$$\begin{cases} \tilde{x}_{k+1}^e = \sum_{i=1}^n \alpha_i(k) (A_i^e \tilde{x}_k^e + B_i^e \tilde{u}_k + W_i^e w_k) \\ \tilde{z}_k = C_{zi}^e \tilde{x}_k^e \end{cases} \quad (4)$$

where

$$A_i^e = \begin{bmatrix} A_i & 0 \\ -t_e C_{zi} & I \end{bmatrix}, B_i^e = \begin{bmatrix} B_i \\ 0 \end{bmatrix}, W_i^e = \begin{bmatrix} W_i \\ 0 \end{bmatrix},$$

$$C_{zi}^e = [C_{zi} \ 0], x_k^e = \begin{pmatrix} \tilde{x}_k \\ x_k^{int} \end{pmatrix}$$

The expression of the discrete time controller for the previous switched system is of the following form:

$$\tilde{u}_k = - \sum_{i=1}^n \alpha_i(k) K_i^e \tilde{x}_k^e \quad (5)$$

The considered control problem is formulated as follows.

Problem: Considering the extended switched model (4) and the switched H_∞ controller (5), find the gains K_i^e such that:

- S1: The closed loop system $\tilde{x}_{k+1}^e = (A_i^e - B_i^e K_i^e) \tilde{x}_k^e$ is globally asymptotically stable when $w_k = 0$.
- S2: The closed loop transfer function $G_{zw}(z)$ from w_k to the controlled output \tilde{z}_k guarantees the H_∞ constraint $\|G_{zw}(z)\|_\infty < \gamma$, $\gamma > 0$.

Theorem: Switching H_∞ controller gain

For $i, j \in 1, 2, \dots, n$, if the pair (A_i^e, B_i^e) is stabilizable for all i , if there exist matrices $Q_i \in \mathbb{R}^{q \times q}$, with $q = m + h$,

positive definite and symmetric and, $U_i \in \mathbb{R}^{q \times p}$ such that the following LMI is verified for all (i, j) :

$$\begin{bmatrix} -Q_i & 0 & (A_i^e Q_i - B_i^e U_i)^T & Q_i C_{zi}^{eT} \\ * & -\gamma^2 I & W_i^{eT} & 0 \\ * & * & -Q_j & 0 \\ * & * & * & -I \end{bmatrix} < 0$$

then, the discrete time switched H_∞ controller (5) of system (3) solves the problem and the gains are given by $K_i^e = U_i Q_i^{-1}$.

Proof: The proof is similar to the existing results presented in Daafouz et al. [2002] and Koenig and Marx [2009].

To establish sufficient conditions to design the controller satisfying the previous specifications:

$$V_{k+1} - V_k + \tilde{z}_k^T \tilde{z}_k - \gamma^2 w_k^T w_k < 0 \quad (6)$$

for all k , where $V_k = \tilde{x}_k^T P_k \tilde{x}_k > 0$ is a candidate Lyapunov function, with $P_k = P_k^T$ and $P_k > 0$, $P \in \mathbb{R}^{q \times q}$.

Let $P_i = P_k$ and $P_j = P_{k+1}$, the difference (6) along the solution of the closed loop system becomes:

$$\begin{pmatrix} \tilde{x}^e \\ w \end{pmatrix}^T \begin{pmatrix} M_{11} & (A_i^e - B_i^e K_i^e)^T P_j W_i^e \\ * & W_i^{eT} P_j W_i^e - \gamma^2 I \end{pmatrix} \begin{pmatrix} \tilde{x}^e \\ w \end{pmatrix}$$

With: $M_{11} = (A_i^e - B_i^e K_i^e)^T P_j (A_i^e - B_i^e K_i^e) - P_i + C_{zi}^{eT} C_{zi}^e$.

Using Schur's complement:

$$\begin{bmatrix} -P_i & 0 & (A_i^e - B_i^e K_i^e)^T & C_{zi}^{eT} \\ * & -\gamma^2 I & W_i^{eT} & 0 \\ * & * & -P_j^{-1} & 0 \\ * & * & * & -I \end{bmatrix} < 0$$

Pre-multiplying by:

$$\begin{bmatrix} P_i^{-1} & 0 & 0 & 0 \\ * & I & 0 & 0 \\ * & * & I & 0 \\ * & * & * & I \end{bmatrix}^T$$

and post-multiplying by:

$$\begin{bmatrix} P_i^{-1} & 0 & 0 & 0 \\ * & I & 0 & 0 \\ * & * & I & 0 \\ * & * & * & I \end{bmatrix}$$

The inequality is equivalent to:

$$\begin{bmatrix} -Q_i & 0 & (A_i^e Q_i - B_i^e U_i)^T & Q_i C_{zi}^{eT} \\ * & -\gamma^2 I & W_i^{eT} & 0 \\ * & * & -Q_j & 0 \\ * & * & * & -I \end{bmatrix} < 0$$

With $Q_i = P_i^{-1}$ and $U_i = K_i^e Q_i$.

A robust H_∞ state feedback controller is designed with a level disturbance attenuation γ for $\|w_k\| \leq 1$, and to ensure operating points tracking, an integrator is added.

As a remark, pole placement can be used as a way to improve the performances of the controller. To force pole

assignment in a sub-region described by a circle of center σ and a radius r , the matrices A_i^e and B_i^e are replaced by $\frac{A_i^e - \sigma I}{r}$ and $\frac{B_i^e}{r}$, respectively in the LMI to solve for controller synthesis (see Montagner et al. [2003] for further details).

3.3 H_∞ Performance Analysis

In this section, the closed-loop system robustness performance is studied. Unique matrices for each subsystems W and C_z describe the unknown input and the controlled output, let $W_i = W = [0 \ 10^3 \ 0]^T$ and $C_{zi} = C_z = [0 \ 0 \ 1]$.

Solving the LMI described in the previous theorem, the designed controller guarantees the H_∞ constraint $\|G_{zw}(z)\|_\infty < \gamma$ with an attenuation rate γ of 0.67.

The following figure shows the Bode diagram of singular value of $G_{zw}(z) = C_z^e (zI - (A_i^e - B_i^e K_i^e))^{-1} W^e$ showing the transfer w to \tilde{z} for each activated subsystems during the simulation scenario presented in the last paper section.

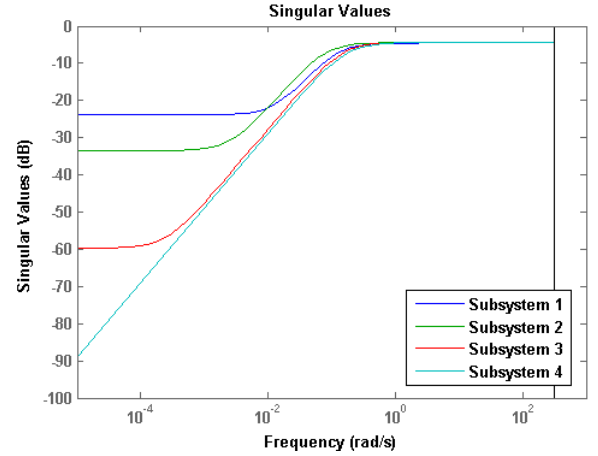


Fig. 5. Bode diagram of the transfer: w to \tilde{z} for each activated subsystems

The disturbance signal is rejected along all the frequency range, with the worst case above all subsystems attenuation value of -3.47 dB corresponding to $20\log(\gamma)$, as expected (Fig.5),

4. APPLICATION: AIR PATH PRESSURES CONTROL

In this section, the results of the switching robust H_∞ controller are presented. Pressure control result of the studied system is presented, showing that the controller satisfied $S1$ and $S2$.

Let $x = [P_1, P_2, P_3]$, $u = [\theta_{thr}, \theta_{byp}]$, $z = P_3$ and $z_{ref} = P_{3sp}$, denoting respectively the states, the control inputs, the controlled output and the reference value.

Controller is validated by simulation with the nonlinear model of the air path system. Reference signal P_{3sp} is a step and varies between low load value $P_{3sp} = P_{atm}$ and high load value $P_{3sp} = 1.01$ bar at an engine speed

N of 2000 RPM (note that due to actuator characteristic maximum load is achieved for $\theta_{thr} = 40\%$ and $\theta_{byp} = 0\%$). Fig.6 shows the results of controlled pressures signals (red, dashed). P_1 and P_2 are compared with the nonlinear model ("NL model") data in open loop (blue, solid). P_3 is compared to the reference signal P_{3sp} (green, solid).

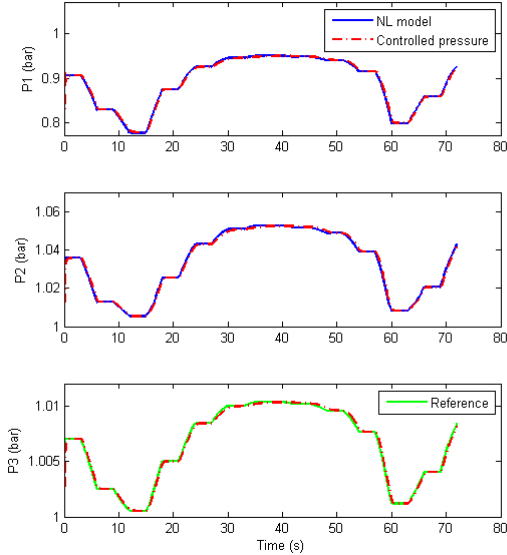


Fig. 6. Reference tracking at N=2000 RPM

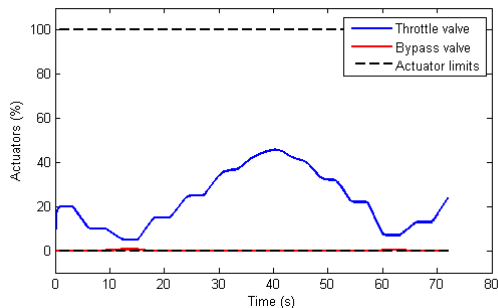


Fig. 7. Control signals during reference tracking at N=2000 RPM (Throttle: blue, Bypass: red)

The reference signal varies from low to high load showing that the controller is stable.

Fig.6 shows that the controller has a good tracking performance. Neither the switching rules, nor the unmodeled dynamics or model approximation error affect the control of the air-path system over all the operating range. Moreover, Fig.7 shows that control inputs meet actuators constraints, avoiding saturation and signal undershoot or overshoot. It is important for the controller to avoid signal peaks. Indeed, short pressure variation alter the driver comfort since brutal excess air increase quickly the torque provoking jolts in car. The same precaution is applied on control input overshoot since it is dangerous for the mechanical system. In other words, compromise between driver comfort and actuator excitation has to be found.

5. CONCLUSION

In this paper, a H_∞ state feedback control for switched linear system is treated. A switched linear state space representation of the air path simplified model by considering that slow dynamics are quite constant has been validated. The extended system performance analysis have shown the accuracy of the proposed approach for unknown input rejection.

Successful application of the pressure tracking shows that the switched control can be an interesting way to deal with highly nonlinear systems control and the implementation issues.

REFERENCES

- J. Daafouz, P. Riedinger, and C. Iung. Stability analysis and control synthesis for switched systems: a switched lyapunov function approach. *IEEE Transactions on Automatic Control*, 47(11):1883 – 1887, November 2002.
- L. Guzzella and C.H. Onder. *Introduction to Modeling and Control of Internal Combustion Engine Systems*. Springer, 2004.
- J.B. Heywood. *Internal Combustion Engine Fundamentals*. McGraw-Hill, 1988.
- D. Ichalal, B. Marx, J. Ragot, and D. Maquin. State estimation of takagi-sugeno systems with unmeasurable premise variables. *IET Control Theory and Applications*, 4:897–908, 2010.
- D. Ichalal, B. Marx, D. Maquin, and J. Ragot. Observer design and fault tolerant control of takagi-sugeno nonlinear systems with unmeasurable premise variables. In *Fault Diagnosis in Robotic and Industrial Systems*, 2012.
- M. Iwadare, M. Ueno, and S. Adachi. Multi-variable air-path management for a clean diesel engine using model predictive control. *SAE International*, January 2009.
- D. Koenig and B. Marx. h_∞ -filtering and state feedback control for discrete-time switched descriptor systems. *IET Control Theory and Applications*, 3(06):661–670, 2009.
- T. Leroy, J. Chauvin, and N. Petit. Airpath control of a si engine with variable valve timing actuators. In *American Control Conference*, 2008.
- Vinicius F. Montagner, Valter J.S. Leite, and Pedro L.D. Peres. Discrete-time switched systems: Pole location and structural constrained control. *IEEE Conference on Decision and Control*, pages 6242 – 6247, December 2003.
- P. Moulin and J. Chauvin. Analysis and control of the air system of a turbocharged gasoline engine. In *Proc. of the 47th IEEE Conference on Decision and Control*, 2008.
- A. T. Nguyen, J. Lauber, and M. Dambrine. Robust h_∞ control design for switching uncertain system: Application for turbocharged gasoline air system control. In *51st IEEE Conference on Decision and Control*, 2012a.
- A. T. Nguyen, J. Lauber, and M. Dambrine. Switching fuzzy control of the air system of a turbocharged gasoline engine. In *Proc. of the IEEE Inter. Conf. on Fuzzy Syst.*, 2012b.